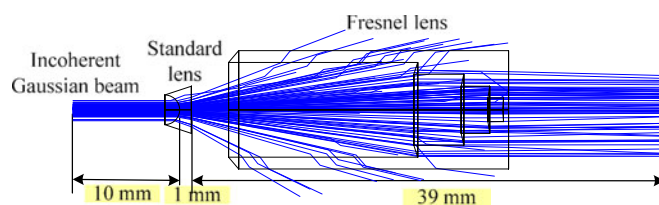
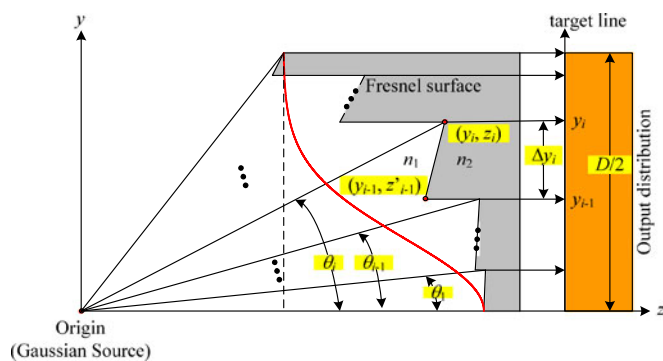


Uniformity and Collimation of Incoherence Gaussian Beam With Divergence Based on Only One Fresnel Surface

Volume 6, Number 8, December 2016

C. M. Tsai



Uniformity and Collimation of Incoherence Gaussian Beam With Divergence Based on Only One Fresnel Surface

C. M. Tsai

Graduate Institute of Precision Engineering, National Chung Hsing University,
Taichung 402, Taiwan R.O.C.

DOI:10.1109/JPHOT.2016.2626474

1943-0655 © 2016 IEEE. Translations and content mining are permitted for academic research only.
Personal use is also permitted, but republication/redistribution requires IEEE permission.
See http://www.ieee.org/publications_standards/publications/rights/index.html for more information.

Manuscript received September 15, 2016; revised October 31, 2016; accepted November 4, 2016.
Date of publication November 8, 2016; date of current version November 28, 2016. This work was supported by the Ministry of Science and Technology, Taiwan, under MOST 104-2622-E-005-019-CC3 and MOST 105-2221-E-005-043. Corresponding author: C.-M. Tsai (e-mail: jmuttsai@gmail.com).

Abstract: An incoherence Gaussian beam with divergence is converted to uniformity and collimation simultaneously at a desirable spot size requirement by using one Fresnel surface. The design process is simplified to one-dimension (1-D) with respect to the incoherence Gaussian beam having revolution symmetry. Such a 1-D Gaussian profile is divided into several parts from the center to the outside. The divided power corresponds to a height difference, i.e., to provide uniformity, the power to the corresponding height difference ratio is constant. The ray passing through the boundary of each part is regarded as the incident ray that would be refracted to run parallel to the optical axis through a piece of surface designed for implementing collimation. An incoherence collimated Gaussian beam is demonstrated to verify the conversion beam with uniformity and collimation simultaneously. The simulation results show that the uniformity is around 95% and the collimation is less than 0.1° .

Index Terms: Beam shaping, uniformity, collimation.

1. Introduction

Increasingly more beam applications are available these days, but such initial beam profiles are not appropriate to use directly in applications. A beam shaping system, therefore, is placed behind the beam source to convert the power distribution into a desirable profile such as uniformity [1], [2]. However, most of the application profiles (e.g., projector light source) are often required to produce uniformity and collimation simultaneously. This is the difficulty of the beam shaping design to result some optimizations [3] developed in uniformity and collimation.

The beam shaping always employs two surfaces, for uniformity and keeping the same optical path length (OPL) [4]–[7]. One surface is responsible for uniformity and the other for OPL keeping all the rays the same. The detector plane is placed behind these two surfaces. When one surface is employed to convert the power distribution into uniformity at the detector plane, the other surface, responding to all the rays on the same OPL tends to destroy the uniformity at the detector plane. Modifying the surfaces for the sake of uniformity would lead all the rays to be unequal on the OPL. Therefore, these two surfaces affect the uniformity and OPL of each other.

The common beam shaping system [4]–[7] is based on the beam source with a Gaussian power profile and collimation to derive the formulas of two aspherical surfaces, in the interests

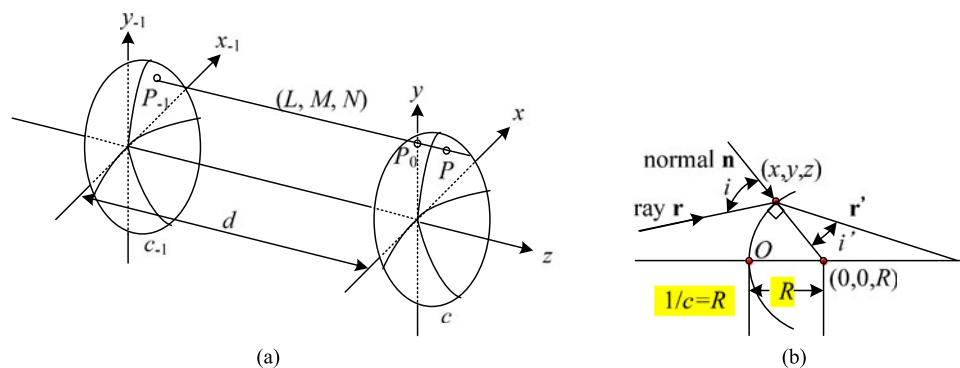


Fig. 1. Ray tracing (a) transference between two spherical surfaces [12] and (b) refraction at a spherical interface [13].

of uniformity and keeping the same OPL. Such a derivation could be limited from that the beam source must be collimated. A beam source with divergent or convergent emission could make it more difficult to obtain a desirable output profile. Recently, laser diodes have become popular for various applications. Serkan and Kirkici [8], [9] derived two aspherical lenses to reshape a divergent elliptical Gaussian laser beam into a circular, collimated and uniform beam. However, the method cannot simultaneously transform the beam source into uniformity and collimation.

Another beam shaping system is based on the Fresnel lens [10], [11] to convert the profile. Campillo *et al.* [10] investigated the Fresnel diffraction by circular apertures for beams commonly encountered in high-power laser systems. Rastani *et al.* [11] proposed a planar Fresnel microlenses to focus, collimate, and bend the individual laser beam. In this paper, either a collimated or a divergent beam source, however, can transform the Gaussian profile into uniformity and collimation simultaneously if the proposed method is applied. The demonstration of the proposal employs an incoherent Gaussian collimated beam that is based on a negative lens to expand the beam to a desirable spot size. As a result, a Fresnel surface with respect to the expanded beam profile is designed to give uniformity and collimation at the detector. The paper is organized as follows. Section 2 describes the ray tracing in a standard lens for beam power distribution. Section 3 illustrates how to construct a Fresnel surface for uniformity and collimation simultaneously. The simulation results are discussed in Section 4. Section 5 concludes this paper.

2. Beam Power Redistribution with Standard Lens

Beam shaping is undertaken to modify the power to meet a desirable power distribution. The size of the original power distribution is always different from that of the application requirements so that a standard lens is often employed to adjust the power distribution. A beam passing through the standard lens can apply the ray tracing method to estimate its new power distribution. The proposal applies two ray tracing processes. One is the transference process, and the other is refraction process [12], [13].

2.1 Transference for Real Ray Tracing

The standard lens consists of two spherical surfaces. A real ray transfers between these two spherical surfaces with the same material. Fig. 1(a) shows a ray transfer from the left spherical surface to the right spherical surface. There are two local rectangle coordinates with respect to these two spherical surfaces. The distance between these two local coordinates (or the thickness of the lens) is d . The intersection point of the ray and the left spherical surface is $P_{-1} = (x_{-1}, y_{-1}, z_{-1})$. This ray following the direction cosine (L, M, N) would propagate to the x - y plane of the right spherical surface at point $P_0 = (x_0, y_0, z_0)$, which is presented by the point P_{-1} , thickness d and

direction cosine (L, M, N) as

$$x_0 = x_{-1} + L (d - z_{-1}) / N \quad (1a)$$

$$y_0 = y_{-1} + M (d - z_{-1}) / N \quad (1b)$$

$$z_0 = 0. \quad (1c)$$

The ray finally transfers to the right spherical surface at the point $P = (x, y, z)$, that is

$$x = x_0 + L\Delta \quad (2a)$$

$$y = y_0 + M\Delta \quad (2b)$$

$$z = N\Delta \quad (2c)$$

where Δ will be derived later. The z shown in (2c) can also be represented as

$$z = 1/2c(x^2 + y^2 + z^2) \quad (3)$$

where c is the radius curvature of the right spherical surface. From (2) and (3), we can obtain

$$1/2c\{(x_0 + L\Delta)^2 + (y_0 + M\Delta)^2 + N^2\Delta^2\} = N\Delta \quad (4)$$

or

$$c^2\Delta^2 - 2c\{N - c(Lx_0 + My_0)\}\Delta + c^2(x_0^2 + y_0^2) = 0 \quad (5)$$

where $c(x_0^2 + y_0^2)$ is defined as F , and $N - c(Lx_0 + My_0)$ is defined as G . The Δ shown in (2) is finally expressed as

$$\Delta = (G \pm (G^2 - cF)^{1/2}) / c \quad (6)$$

or

$$\Delta = \frac{F}{G + \sqrt{G^2 - cF}} \quad (7)$$

A ray transference process beginning from the point P_{-1} located on the left spherical surface can apply (1), (2), and (7) in order to find the point P located on the right spherical surface. Although (6) can also be used to find the Δ during the transference process, the difference between the term G^2 and the term cF is very great, resulting in a problem of numerical precision when running the simulation. Therefore, (7) is always applied in the transference process instead of (6) to improve the numerical precision.

2.2 Refraction for real ray tracing

A ray transfers in the same material, but it refracts at an interface between two different materials. Fig. 1(b) shows a ray refracting at the spherical interface from one material with a refractive index n to another material with a refractive index n' . The incident and the refractive rays are regarded as unit vectors $\mathbf{r} = (L, M, N)$ and $\mathbf{r}' = (L', M', N')$, respectively. Connecting the intersection point of the incident ray and the refractive ray to the center of the sphere is a normal line, which is expressed as a unit vector \mathbf{n} . The relation for the incident ray, refractive ray and normal line obeys Snell's law, namely

$$n'(\mathbf{r}' \times \mathbf{n}) = n(\mathbf{r} \times \mathbf{n}) \quad (8)$$

Using the vector \mathbf{n} cross product to (8), we find

$$n'\mathbf{r}' - n\mathbf{r} = [n'\cos(i') - n\cos(i)]\mathbf{n} \quad (9)$$

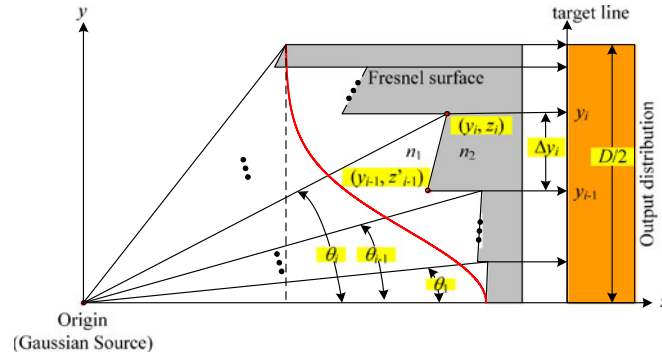


Fig. 2. Fresnel surface design for uniformity and collimation simultaneously.

where i' and i are the incident and refractive angles, respectively, as shown in Fig. 1(b). The normal vector \mathbf{n} in the spherical surface can be represented as

$$\mathbf{n} = (-cx, -cy, 1 - cz) \quad (10)$$

where c is the radius curvature of the spherical surface, and (x, y, z) is the intersection point of the incident ray and refractive ray. Given the incident ray $\mathbf{r} = (L, M, N)$ and normal line $\mathbf{n} = (-cx, -cy, 1 - cz)$, the refractive vector $\mathbf{r}' = (L', M', N')$ is found by applying (9). When a standard lens is employed to adjust the power distribution, using the transference and refraction processes can estimate the new power distribution. However, the standard lens is often employed to expand the size of the Gaussian beams.

3. Fresnel Surface Design to Convert Incoherence Gaussian Beam into Uniformity and Collimation

Although the standard lens can modify the power distribution, it is difficult, using only one standard lens, to produce uniformity and collimation simultaneously. A scheme is proposed to make a beam with a divergent Gaussian profile to produce uniformity and collimation simultaneously through only one Fresnel surface design, as shown in Fig. 2. The original source is the required divergence. If the original source is collimated or has very small divergence, a standard lens can be placed behind the source to make it divergent. The rays of the divergent source would propagate from the material with the refractive index n_1 into the designed Fresnel surface with the material with the refractive index n_2 to realize uniformity and collimation simultaneously.

The plan of uniform distribution is to organize the partial power distribution of the original Gaussian profile into an appropriate height difference. The Gaussian profile is presented as

$$I = I_0 e^{-2(\frac{\theta}{\sigma})^2} \quad (11)$$

where I_0 is the central irradiance, θ is the divergent angle, and σ is the variance. It is necessary to divide the original power distribution into several parts N with the power

$$P(i) = \int_{\theta_{i-1}}^{\theta_i} I_0 e^{-2(\frac{\theta}{\sigma})^2} d\theta \quad \text{for } i = 1, 2, \dots, N \quad (12)$$

where $\theta_0 = 0$, and θ_N is the boundary of the source. Two divergent rays with divergent angles θ_{i-1} and θ_i would pass at the heights y_{i-1} and y_i to form the height difference Δy_i , as shown in Fig. 2. The initial height, y_0 , is zero. When the divided power to the height difference Δy_i ratio at the target line is constant, that is,

$$\frac{P(i)}{\Delta y_i} = \text{const} \quad \text{for } i = 1, 2, \dots, N \quad (13)$$

we can obtain uniform distribution. However, (13) is one of the conditions of this uniform distribution. It cannot form uniformity without collimation. The collimation method is follows Snell's law [14]

$$[1 + n_r^2 - 2n_r(\mathbf{O} \cdot \mathbf{I})]^{1/2} \mathbf{N} = \mathbf{O} - n_r \mathbf{I} \quad (14)$$

where $n_r = n_1/n_2$ and \mathbf{I} , \mathbf{O} , \mathbf{N} are the unit vectors for the incident ray, output ray, and normal line, respectively. The output unit vector \mathbf{O} is $[0 \ 0 \ 1]$ for the collimation requirement and the incident unit vector of the ray with divergent angle θ_i is $[0 \ \sin\theta_i \ \cos\theta_i]$. Applying (14), one can find the normal unit vector $\mathbf{N} = [0 \ a \ b]$. In order to make the ray with the divergent angle θ_i collimated, we have to construct a line whose normal unit vector is \mathbf{N} . The relation between the line and the normal unit vector is orthogonal, that is

$$a(y_i - y_{i-1}) + b(z_i - z'_{i-1}) = 0 \quad (15)$$

where y_{i-1} and y_i are found from (13), and z_i is

$$z_i = y_i \tan\theta_i. \quad (16)$$

Using (15), one can find the z'_{i-1} to construct the line for collimation. A simple scheme is presented here to demonstrate the simultaneous uniformity and collimation which separates the same divided power, that is

$$P(i) = \int_{\theta_{i-1}}^{\theta_i} I_0 e^{-2(\frac{\theta}{\sigma})^2} d\theta = \frac{\int_{\theta_0}^{\theta_N} I_0 e^{-2(\frac{\theta}{\sigma})^2} d\theta}{N} \quad \text{for } i = 1, 2, \dots, N. \quad (17)$$

If the desirable diameter of the output distribution is D , the corresponding height difference Δy_i is

$$\Delta y_i = \frac{D}{2N} \quad \text{for } i = 1, 2, \dots, N \quad (18a)$$

and

$$y_i = y_{i-1} + \Delta y_i \quad \text{for } i = 1, 2, \dots, N \quad (18b)$$

where $y_0 = 0$. Notice that the output spot size can be controlled from (18a) by assigning the parameter D . The θ_i is derived from (17) to give the same divided power. Using (14) and the θ_i one can find the normal unit vector \mathbf{N} and the point (y_i, z_i) can be found from (18) and (16). Finally, the z'_{i-1} is found from (15) to construct the line for simultaneous uniformity and collimation.

4. Simulation results and discussions

An incoherent collimated Gaussian beam with beam radius 1.15 mm is used to verify the proposed method. The beam will be expanded to radius 5 mm so that a negative standard lens is placed behind the beam to respond to the ray's divergence. We applied (17) to find the N boundary positions with the same power. These positions are the ray tracing initial points. Using two transference processes and one refraction process, one can find N crossing points on the rear surface of the standard lens. Regarding the rear surface of the standard lens, the Fresnel surface is designed to convert the incoherent Gaussian beam to uniformity and collimation.

The radiuses of the standard lens in the paper are set at -1.25 mm and infinity for the front and rear surfaces, respectively. The thickness of the standard lens is 1 mm. The distance between the incoherent Gaussian beam and the standard lens is 10 mm. Fig. 3 shows the construction of the beam shaping that divides the incoherent Gaussian beam into five parts with the same power. We apply the commercial optical software Zemax to make the simulation. The input power is set at 1 W, and the number of the ray for analysis is 500 million. The number of pixels is set at 1000×1000 at the detector whose size and angle are from -6 mm to 6 mm and -1° to 1° , respectively, when the beam power distribution is divided into five parts with the same power (e.g., $N = 5$).

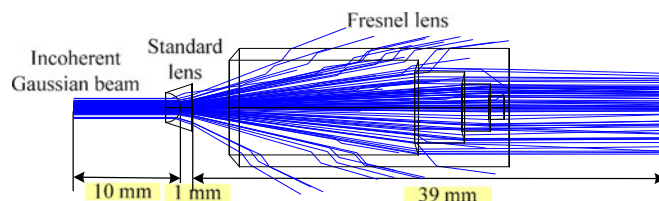


Fig. 3. Construction of the beam shaping.

TABLE I
Point coordinates of the Fresnel lens for $N = 5$

Pair #	1	2	3	4	5	6
Coordinate of point 1 (y, z)	(0, 26.294)	(1, 25.054)	(2, 22.784)	(3, 18.782)	(4, 3.128)	(5, 26.794)
Coordinate of point 2 (y, z)	(1, 26.360)	(2, 25.190)	(3, 23.004)	(4, 19.117)	(5, 3.980)	(0, 26.794)

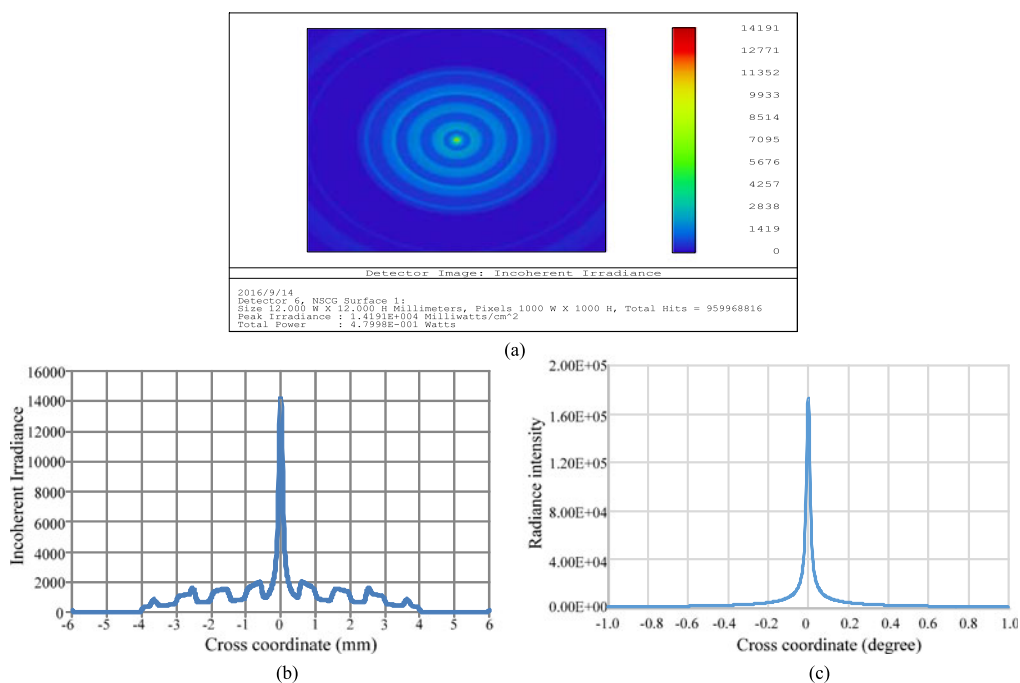


Fig. 4. Simulation result for the five divided parts of the incoherent Gaussian beam. (a) Spot irradiance. (b) Cross section of the spot irradiance. (c) Cross section of the radiance intensity.

Using the proposed method, one can find six pairs of points to construct the Fresnel lens for making the uniformity and collimation simultaneous. The coordinates of the six pairs of points of the Fresnel surface are listed in Table 1.

Fig. 4 shows the simulation result for $N = 5$. The collimation is defined from the angle of full width at half maximum (FWHM). The result shows that the collimation is about 1° . However, the uniformity looks very bad. Still, when one divides the power distribution into more parts and creates more points for the Fresnel surface, the uniformity at the detector can be improved. Moreover,

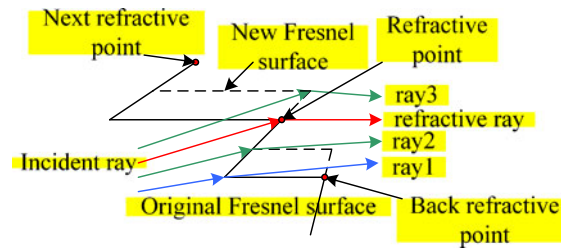
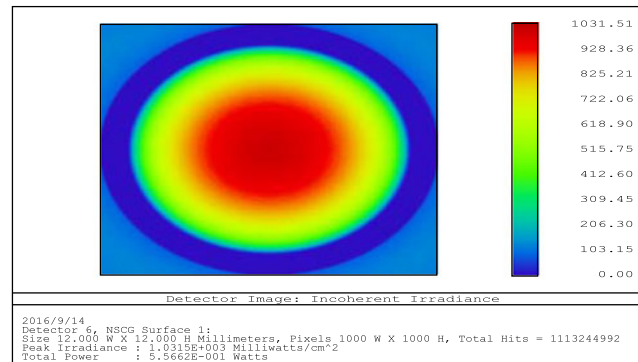
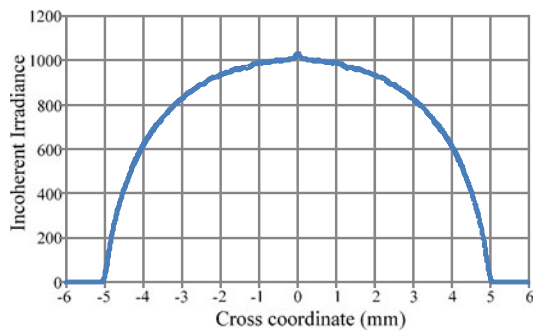


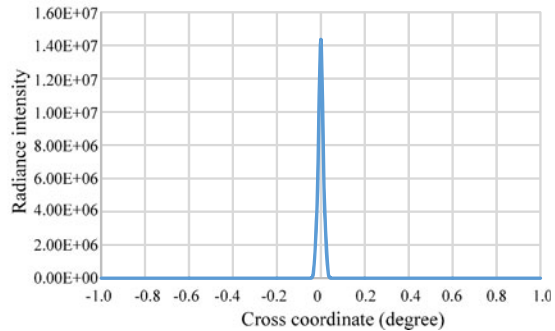
Fig. 5. Modification of the Fresnel surface to produce uniformity and collimation.



(a)



(b)



(c)

Fig. 6. Simulation result of the modified Fresnel surface for the 200 divided parts of the incoherent Gaussian beam. (a) Spot irradiance. (b) Cross section of the spot irradiance. (c) Cross section of the radiance intensity.

recalling the refractive points of the Fresnel surface for collimation, they are located at the end of the segment of the Fresnel surface, as shown in Fig. 5. The refractive ray is the collimated ray. The ray1 shown in Fig. 5 is another refractive ray from the other end of the segment for the original Fresnel surface, making ray1 deviate extremely from the collimation. Therefore, a scheme is presented to modify the Fresnel surface for alleviating the ray's deviation from the collimation. The refractive points are the same; however, the two ends of the segment are different from the original one. The new y of one end of the segment is the coordinate of the refractive point plus half the distance from the refractive point to the next refractive point. We can apply (15) to find the new point for constructing the new Fresnel surface. The dash line shown in Fig. 5 is the new Fresnel surface; it has the result of alleviating the deviation of ray2 and ray3 from collimation. Fig. 6 shows the simulated result of using the modified Fresnel surface. The uniformity is greatly improved and the collimation is less than 0.1° at the detector when the number of divided parts is 200.

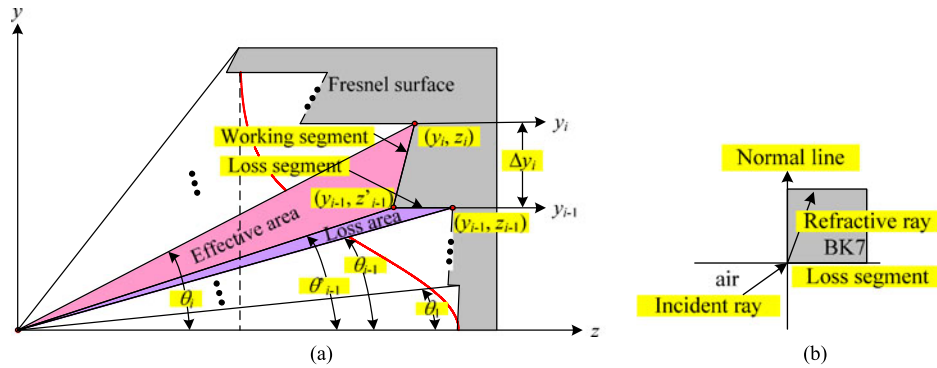


Fig. 7. Designated Fresnel surface about (a) the power distribution and (b) the loss segment.

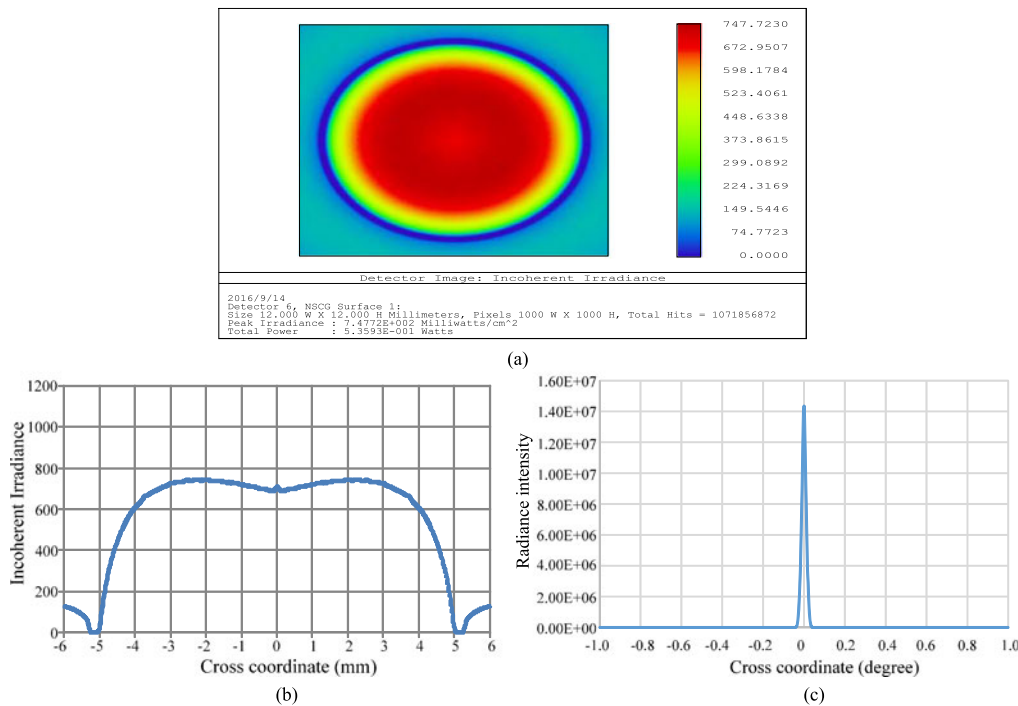


Fig. 8. Simulation result of the hybrid Fresnel surface for the 200 divided parts of the incoherent Gaussian beam. (a) Spot irradiance. (b) Cross section of the spot irradiance. (c) Cross section of the radiance intensity.

The output power from Fig. 6(a) is around 0.556 W at the detector. This implies that there is some power loss during the beam shaping process at the Fresnel surface. Let us observe the Fresnel surface. Fig. 7(a) shows the power distribution at the designed Fresnel surface. The rays between the angles θ'_{i-1} and θ_i would refract through the working segment to propagate at the detector. However, the rays between the angles θ_{i-1} and θ'_{i-1} would refract through the lost segment and cannot arrive at the detector, as shown in Fig. 7(b). Therefore, the lost power comes from the area of loss. It is more severe from the inside to the outside of the Fresnel surface because the lost segment becomes longer and longer. From (13), the condition of the uniformity is that the difference of power over height is constant. When the Fresnel segment has more loss power, it is necessary to adjust the height difference to comply with the uniformity condition. We apply the geometric series to adjust the height difference, which is

$$\Delta y_i = a^{i-1} \Delta y_1 \quad \text{for } i = 1, \dots, N \tag{19a}$$

and

$$\sum_{i=0}^{N-1} a^i \Delta y_1 = D/2 \quad (19b)$$

where a is a real number between 0 and 1, and the coordinate y_i is $\sum_{j=1}^i \Delta y_j$.

A hybrid structure is based on the modified scheme, but the height difference is according to the geometric series adjusted to make the output profile more uniform. One can construct a Fresnel surface that makes the power distribution more uniform at the detector. Fig. 8 shows the simulation result when a is set to 0.998. As can be seen, uniformity is significantly improved through using the geometric series. If we regard half of the width of the power distribution to evaluate the uniformity (that is, referring -2.5 mm to 2.5 mm), it is about 95% of the uniformity for minimum power over maximum power. The collimation is less than 0.1° , and the power efficiency is 53.593%.

5. Conclusions and Future Works

An incoherent Gaussian beam with divergence is converted into uniformity and collimation at a desirable spot size by using only one Fresnel surface. The uniform condition is to make the partial power over height difference constant. It is necessary to divide the beam into several parts. Each part corresponds to a height difference that is regarded as constructing a surface for collimation according to Snell's law. We first averaged the beam power and the height difference to design the Fresnel surface, and later modified the Fresnel surface to balance the deviation of the rays. However, the loss segment of the Fresnel surface leads some rays to deviate extremely from the collimation, with the result that the height difference must be modified to satisfy the uniform condition. Adjusting the height difference on the basis of the geometric series can effectively improve the uniformity at the detector. As a result, only one Fresnel surface is needed to convert the power distribution to simultaneous uniformity and collimation. However, the uniformity and power efficiency can still be improved by modifying the structure of the Fresnel lens. Our future works are to find an approach to fit the segment power into the high difference and to reduce the loss segment as much as possible.

References

- [1] A. X. Cao, H. Pang, J. Z. Wang, M. Zhang, L. F. Shi, and Q. L. Deng, "Center off-axis tandem microlens arrays for beam homogenization" *IEEE Photon. J.*, vol. 7, no. 3, Jun. 2015, Art. no. 2400207.
- [2] D. Wang, B. Q. Jin, Y. Wang, P. Jia, D. M. Cai, and Y. Gao, "Adaptive flattop beam shaping with a spatial light modulator controlled by the holographic tandem method," *IEEE Photon. J.*, vol. 8, no. 1, Feb. 2016, Art. no. 6500107.
- [3] C. M. Tsai, Y. C. Fang, and C. T. Lin, "Application of genetic algorithm on optimization of laser beam shaping," *Opt. Exp.*, vol. 23, no. 12, pp. 15877–15887, Jun. 2015.
- [4] B. R. Frieden, "Lossless conversion of a plane laser wave to a plane wave of uniform irradiance," *Appl. Opt.*, vol. 4, no. 11, pp. 1400–1403, 1965.
- [5] J. A. Hoffnagle and C. M. Jefferson, "Design and performance of a refractive optical system that converts a Gaussian to a flattop beam," *Appl. Opt.*, vol. 39, no. 30, pp. 5488–5499, Oct. 2000.
- [6] S. Zhang, G. Neil, and M. Shinn, "Single-element laser beam shaper for uniform flat-top profiles," *Opt. Exp.*, vol. 11, no. 16, pp. 1942–1948, Aug. 2003.
- [7] C. Liu and S. Zhang, "Study of singular radius and surface boundary constraints in refractive beam shaper design," *Opt. Exp.*, vol. 16, no. 9, pp. 6675–6682, Apr. 2008.
- [8] M. Serkan and H. Kirkici, "Optical beam-shaping design based on aspherical lenses for circularization, collimation, and expansion of elliptical laser beams," *Appl. Opt.*, vol. 47, no. 2, pp. 230–240, Jan. 2008.
- [9] M. Serkan and H. Kirkici, "Reshaping of a Divergent Elliptical Gaussian laser beam into a circular, collimated, and uniform beam with aspherica lens design," *IEEE Sensors. J.*, vol. 9, no. 1, pp. 36–44, Jan./ Feb. 2009.
- [10] A. J. Campillo, J. E. Pearson, S. L. Shapiro, and N. J. Terrell Jr., "Fresnel diffraction effects in the design of high-power laser systems," *J. Appl. Phys.*, vol. 23, pp. 85–85, 1973.
- [11] K. Rastani, M. Orenstein, E. Kapon, and A. C Vonlehmen, "Integration of planar Fresnel microlenses with vertical-cavity surface-emitting laser arrays," *Opt. Lett.*, vol. 16, no. 12, pp. 919–921, Jun. 1991.
- [12] W. T. Welford, *Aberrations of Optical Systems*. Boca Raton, FL, USA: CRC, 1986.
- [13] C. M. Tsai, "Evaluation of geometrical modulation transfer function in optical lens system," *Math. Probl. Eng.*, vol. 2015, 2015, Art. no. 863201.
- [14] K. Wang, S. Liu, F. Chen, Z. Qin, Z. Liu, and X. Luo, "Freeform LED lens for rectangularly prescribed illumination," *J. Opt. A, Pure Appl. Opt.*, vol. 11, Oct. 2009, Art. no. 105501.